

Diabetic Müller-Glial-Cell-Specific *Il6ra* Knockout Mice Exhibit Accelerated Retinal Functional Decline and Thinning of the Inner Nuclear Layer

Joshua Glass,¹ Rebekah L. Robinson,¹ Grace Greenway,¹ Garrett Jones,¹ and Shruti Sharma¹⁻³

¹Center for Biotechnology and Genomic Medicine, Augusta University, Augusta, Georgia, United States

²Culver Vision Discovery Institute, Augusta University, Augusta, Georgia, United States

³Department of Ophthalmology, Augusta University, Augusta, Georgia, United States

Correspondence: Shruti Sharma, Center for Biotechnology and Genomic Medicine, Department of Ophthalmology, Medical College of Georgia, Augusta University, 1120 15th Street, CAII 4139, Augusta, GA 30912, USA; shsharma@augusta.edu.

JG and RLR should be considered co-first authors.

Received: September 11, 2023

Accepted: November 8, 2023

Published: December 1, 2023

Citation: Glass J, Robinson RL, Greenway G, Jones G, Sharma S. Diabetic Müller-glial-cell-specific *Il6ra* knockout mice exhibit accelerated retinal functional decline and thinning of the inner nuclear layer. *Invest Ophthalmol Vis Sci.* 2023;64(15):1. <https://doi.org/10.1167/iovs.64.15.1>

PURPOSE. Interleukin-6 (IL-6) is implicated in the pathology of diabetic retinopathy (DR). IL-6 trans-signaling via soluble IL-6 receptor (IL-6R) is primarily responsible for its pro-inflammatory functions, whereas cis-signaling via membrane-bound IL-6R is anti-inflammatory. Using a Müller-glial-cell-specific *Il6ra*^{-/-} mouse, we examined how loss of IL-6 cis-signaling in Müller glial cells (MGCs) affected retinal thinning and electroretinography (ERG) response over 9 months of diabetes.

METHODS. Diabetes was induced in wildtype and knockout mice with streptozotocin (40 mg/kg, daily for 5 days). Spectral domain optical coherence tomography (SD-OCT), ERG, and funduscopy/fluorescein angiography (FA) were assessed at 2, 6, and 9 months of diabetes. MGCs and bipolar neurons were examined in retinal tissue sections by immunofluorescence.

RESULTS. Diabetic MGC *Il6ra*^{-/-} mice had significantly thinner retinas than diabetic wildtype mice at 2 (-7.6 μm), 6 (-12.0 μm), and 9 months (-5.0 μm) of diabetes, as well as significant thinning of the inner nuclear layer (INL). Diabetic MGC *Il6ra*^{-/-} mice also showed a reduction in scotopic B-wave amplitude and B-wave/A-wave ratio earlier than wildtype diabetic mice. In retinal sections, we found a decrease in bipolar neuronal marker PKCα only in diabetic MGC *Il6ra*^{-/-} mice, which was significantly lower than both controls and diabetic wildtype mice. Glutamine synthetase, a Müller cell marker, was reduced in both wildtype and MGC *Il6ra*^{-/-} diabetic mice compared to their respective controls.

CONCLUSIONS. IL-6 cis-signaling in MGCs contributes to maintenance of the INL in diabetes, and loss of the IL-6 receptor reduces MGC-mediated neuroprotection of bipolar neurons in the diabetic retina.

Keywords: IL-6 trans-signaling, Müller glia, diabetic retinopathy (DR), inner nuclear layer (INL)

Evidence suggests that interleukin-6 (IL-6) plays a prominent role in diabetic retinopathy (DR) pathogenesis.¹⁻⁵ IL-6 functions through multiple signaling modalities, including “classical” or “cis-signaling” through a membrane-bound IL-6 receptor (mIL-6R) and “trans-signaling” through a soluble IL-6 receptor (sIL-6R).⁶⁻⁸ Cis-signaling is therefore limited to cell types that express mIL-6R and is generally believed to mediate the various physiological and regenerative functions of this cytokine.^{6,8-13} In contrast, IL-6 trans-signaling can activate signaling in cells that lack membrane-bound IL-6R, as it only requires the sIL-6R and the ubiquitously expressed IL-6 co-receptor, glycoprotein 130 (gp130).¹⁴ We and others have shown that the downstream effects of this pathway are primarily pro-inflammatory.^{9,11,12,15-17} In the retina, IL-6 has been shown to have both beneficial and detrimental effects. IL-6 is neuroprotective in ischemia, retinal detachment, elevated intraocular pressure, and hyperglycemia,¹⁸⁻²³ yet we and others have

also observed IL-6 induced damage involving retinal oxidative stress and vascular dysfunction.^{16,24-26}

Although cells that do not express mIL-6R can only be activated by sIL-6R through trans-signaling, those cell types that express the membrane-bound form of the receptor can be activated by both cis- and trans-signaling pathways, allowing for diverse functionality of IL-6 in tissues. The preferential activation of one IL-6 pathway over the other is thought to be controlled by the ratio of free IL-6 to IL-6/sIL-6R complexes in circulation, in a homeostatic relationship that can be described as an “IL-6 cis-trans balance.” The principal glial cell type in the retina, Müller glial cells (MGCs), express the membrane bound IL-6 receptor and, therefore, are sensitive to disruption of the cis-trans balance. MGCs are the only cells that span the entire width of the retina and thus have intimate contact with retinal blood vessels and nearly all retinal cell types.²⁷⁻²⁹ MGCs interact with endothelial cells (ECs), which we have



shown do not express mIL-6R,¹⁶ to regulate the tightness of the blood retinal barrier (BRB)^{6,29-34} and retinal angiogenesis.³⁵ Glial and vascular cells work together to provide critical metabolic and structural support to the delicate retinal tissue, and hyperglycemia-induced dysfunction of these cell types contributes to DR pathogenesis.^{27,36-43} Thus, characterizing the roles of IL-6 cis- and trans-signaling in both the function of MGCs and their interactions with retinal ECs is critical for the development of new therapies targeting the IL-6 pathway. An earlier study has shown that IL-6 cis-signaling in MGCs mediates neuroprotection through upregulation of vascular endothelial growth factor A (VEGFA),¹⁸ although the full effects of this pathway in vivo have not been characterized.

We have recently generated a novel Müller-glial-cell-specific knockout mouse that does not express the mIL-6R in MGCs and can therefore serve as a “trans-signaling-only” model to identify the specific effects resulting from the loss of IL-6 cis-signaling in MGCs in DR.⁴⁴ Here, we describe the longitudinal changes to retinal function and architecture over 2 to 9 months of streptozotocin (STZ)-induced diabetes relative to wildtype mice. Our studies show that loss of IL-6 cis-signaling in MGCs leads to earlier inner nuclear layer (INL) thinning, electroretinography (ERG) changes, and loss of bipolar neurons, suggesting that IL-6 cis-signaling in MGCs may play a novel functional and neuroprotective role in DR.

METHODS

Animal Studies

All animal studies were conducted in accordance with the ARVO Statement for the Use of Animals in Ophthalmic and Vision Research and the Animal Research: Reporting of In Vivo Experiments (ARRIVE) guidelines. At 6 to 8 weeks of age, diabetes was induced in C57BL/6J mice (Jackson Laboratory, Bar Harbor, ME, USA) and MGC *Il6ra*^{-/-} mice⁴⁴ by intraperitoneal injection of 40 mg/kg streptozotocin (Sigma, St. Louis, MO, USA) in sodium citrate buffer (0.05 M, pH 4.5) once daily for 5 days. Body weight and blood glucose were measured at 2-week intervals throughout the course of the study, and mice were considered diabetic when glucose levels were consistently above 250 mg/dL. Age-matched non-diabetic controls for each strain were maintained and housed with diabetic mice. Retinal architecture and function were assessed after 2, 6, and 9 months of diabetes, as described below, and, at the conclusion of the study period, all mice ($n = 18-34$ /group) were humanely euthanized. Whole eyes were collected for molecular and immunofluorescence studies. All resources and efforts were used to ensure the safe and humane treatment of animals used in the study to minimize any possible suffering during experimental procedures and euthanasia. The animal protocol (Protocol #2014-0676) was approved by the Institutional Animal Care and Use Committee (IACUC) at Augusta University.

Funduscopy and Fluorescein Angiography

Retinal imaging was performed in anesthetized mice using a Phoenix MICRON IV imaging system (Bend, OR, USA). Fundoscopic imaging was conducted in bright field mode, after which the mice were administered a subcutaneous injection of fluorescein dye (10 μ L; AK-FLUOR 10%, 100

mg/mL). For fluorescein angiography (FA) imaging, brightness and image exposure were kept consistent for all mice to enable accurate image comparisons.

Spectral Domain Optical Coherence Tomography

At 2, 6, and 9 months of diabetes, mice were anesthetized with ketamine (80 mg/kg) and xylazine (16 mg/kg), pupils dilated with 1% tropicamide ophthalmic solution (Akorn, Inc., Lake Forest, IL, USA), and the eyes were lubricated with GenTeal Tears PF Lubricant Moderate Eye Drops (Alcon Laboratories, Inc., Fort Worth, TX, USA) prior to imaging. Segmentation and measurements of individual retinal layer thickness were obtained on a Bioptigen Spectral Domain Ophthalmic Imaging System (SDOIS; Bioptigen System Envisu-R2200, Durham, NC, USA) and analyzed using the InVivoVue™ Diver 2.4 software (Bioptigen, Inc.).

Electroretinography

Dark-adapted mice were anesthetized as above, and pupils were dilated with 1% tropicamide ophthalmic solution (Akorn, Inc.) and 2.5% phenylephrine-hydrochloride ophthalmic solution (Akorn, Inc.). Scotopic and photopic A-wave and B-wave amplitudes (μ V) from both eyes were recorded over increasing flash intensities (0.001, 0.005, 0.01, 0.1, 0.5, and 1.00 cds/m² [scotopic response]; and 25, 50, 100, and 150 cds/m² [photopic]) using a Celeris Full-Field Stimulator, and average amplitude values were calculated using Diagnosys Espion software (Diagnosys LLC, Lowell, MA, USA).

Immunofluorescence

Immediately following euthanasia, whole eyes were dissected and embedded in Tissue-Tek OCT compound (Sakura Finetek USA, Torrance, CA, USA), flash frozen in a dry ice-ethanol slurry, and stored at -80°C until further analysis. For immunofluorescence, retinal sections were incubated overnight with anti-PKC α antibody (A13342; ABclonal, Woburn, MA, USA; 1:100) and anti-GS (glutamine synthetase) antibody (MA5-27749; Invitrogen, Carlsbad, CA, USA; 1:100), followed by the appropriate secondary antibody conjugated to Alexa Fluor 488 or Alexa Fluor 546 (Invitrogen) for 1 hour at room temperature. Nuclei were counterstained with DAPI, and fluorescent images were captured with a Leica STELLARIS confocal microscope at 20 \times or 40 \times magnifications. In each image, fluorescence intensity was measured as integrated pixel density with ImageJ software (National Institutes of Health [NIH]), and the mean fluorescence intensity value for each mouse was determined using at least six individual images.

Statistical Analysis

Statistical analyses were performed with GraphPad Prism software 9.0 (GraphPad Software, Inc., San Diego, CA, USA) using 2-way ANOVA with Tukey's multiple comparison's test, considering disease state (control versus diabetic) and genotype (wildtype versus MGC *Il6ra*^{-/-}) as independent variables. Data from each experimental time point were analyzed independently. Any P values < 0.05 were considered for determination of statistical significance.

RESULTS

Body Weight and Blood Glucose Levels in Wildtype and MGC *Il6ra*^{-/-} Mice

Body weight and blood glucose were monitored biweekly in all groups, and all STZ-injected animals were diabetic within 2 weeks following injections. There were no significant

differences in blood glucose levels between genotypes in either the diabetic groups or the age-matched controls (Fig. 1).

Qualitative Assessment of Retinal Lesions and Vascular Changes in Wildtype and MGC *Il6ra*^{-/-} Mice

As a qualitative assessment of retinal lesions and vascular changes between genotypes, funduscopy and FA images were taken at 2, 6, and 9 months of diabetes in all groups (Fig. 2). Abnormal blood vessels were seen in both wildtype and MGC *Il6ra*^{-/-} retinas at 6 and 9 months of diabetes, including increased vessel tortuosity, vessel dilation and vascular beading, and leakage of fluorescein.

Diabetic MGC *Il6ra*^{-/-} Mice Show Accelerated Retinal Thinning and Inner Nuclear Layer Volume Loss

SD-OCT and retina layer segmentation measurements were taken in both eyes of all mice at 2, 6, and 9 months of diabetes to assess changes to retinal thickness and evaluate the specific contribution of each retinal layer to overall change. In wildtype mice, total retinal thickness was unchanged after 2 months yet significantly reduced after 6 months (-7.6 μm, P = 0.026 versus control) and 9 months (-12.7 μm, P < 0.001 versus control) of diabetes (Fig. 3A). In contrast, total retinal thickness in MGC *Il6ra*^{-/-} mice was decreased after only 2 months of diabetes compared to their controls (-7.0 μm, P = 0.005 versus control) and relative to wildtype diabetics (-7.6 μm, P = 0.002 versus

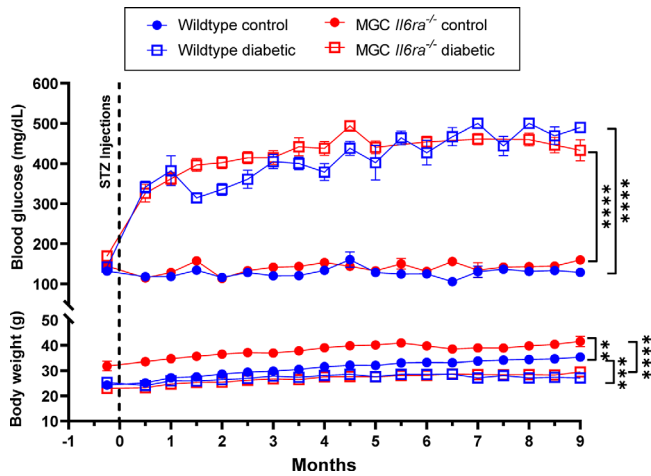


FIGURE 1. Body weight and blood glucose levels in wildtype and MGC *Il6ra*^{-/-} mice. Mouse body weights (g) and blood glucose levels (mg/dL) measured in each group biweekly for the duration of the study (36 weeks). Data are represented as mean ± SEM, n = 18 to 34 mice/group, 6 to 8 weeks of age at diabetes induction; **P < 0.01, ***P < 0.001, ****P < 0.0001.

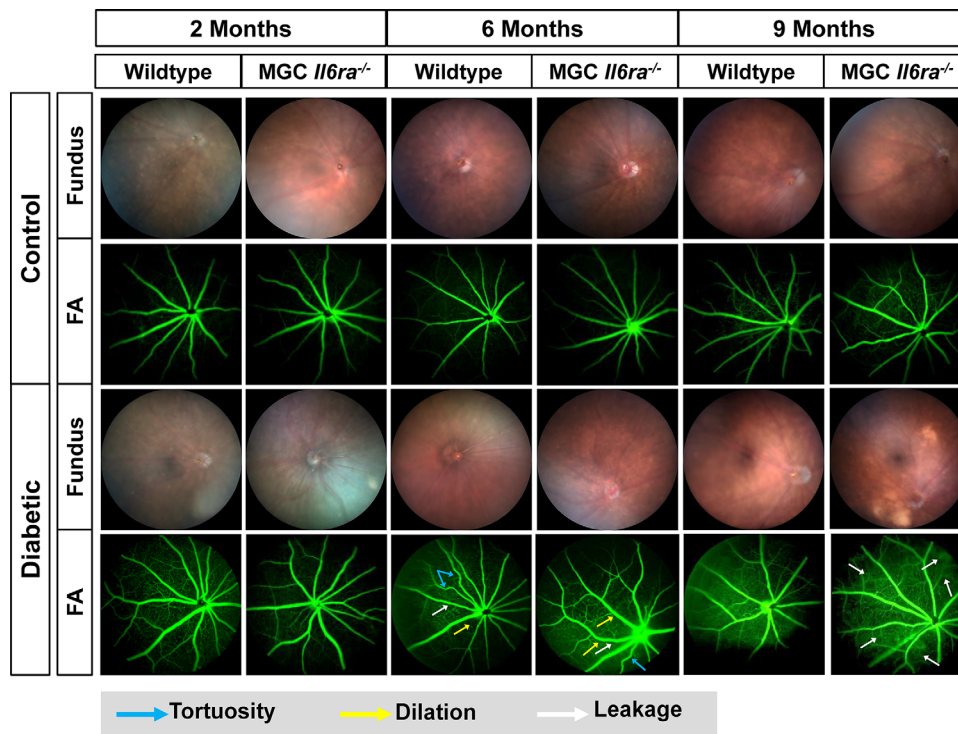


FIGURE 2. Wildtype and MGC *Il6ra*^{-/-} mice show similar vascular changes in late DR. Representative funduscopy and fluorescein angiography (FA) images of control and diabetic retinas at 2-, 6-, and 9-month study time points. Arrows indicate vessel tortuosity (blue), vessel dilation (yellow), and beading or leaky vessels (white).

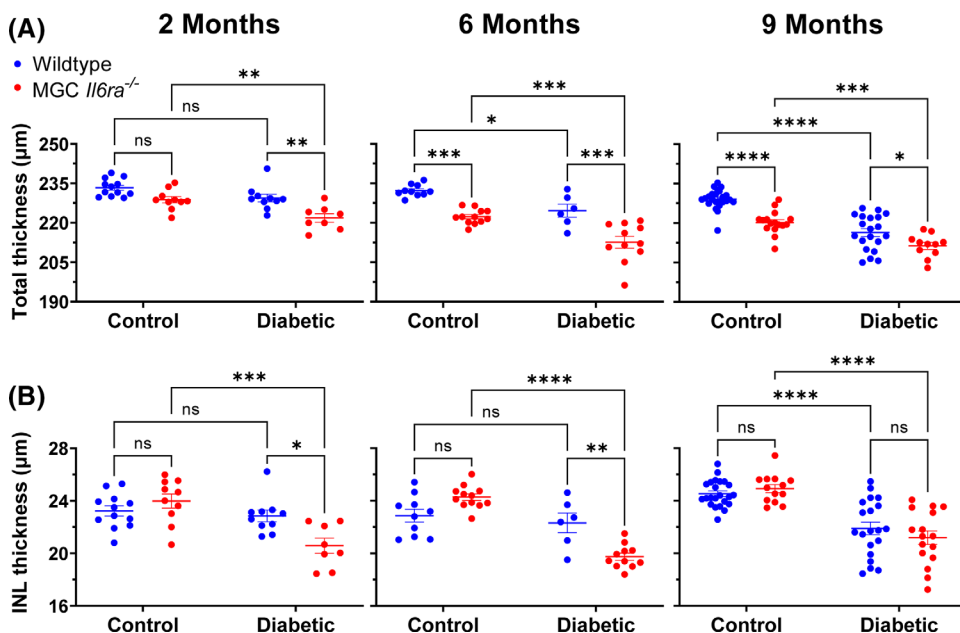


FIGURE 3. Diabetic MGC *Il6ra*^{-/-} mice show accelerated retinal thinning and INL volume loss. (A) Total retinal thickness and (B) INL thickness in wildtype and MGC *Il6ra*^{-/-} mice with and without diabetes at 2, 6, and 9 months. Graphed as mean ± SEM, *n* = 6 to 24 eyes from 3 to 12 mice per time point, per group; **P* < 0.05, ***P* < 0.01, ****P* < 0.001, *****P* < 0.0001; ns = not significant.

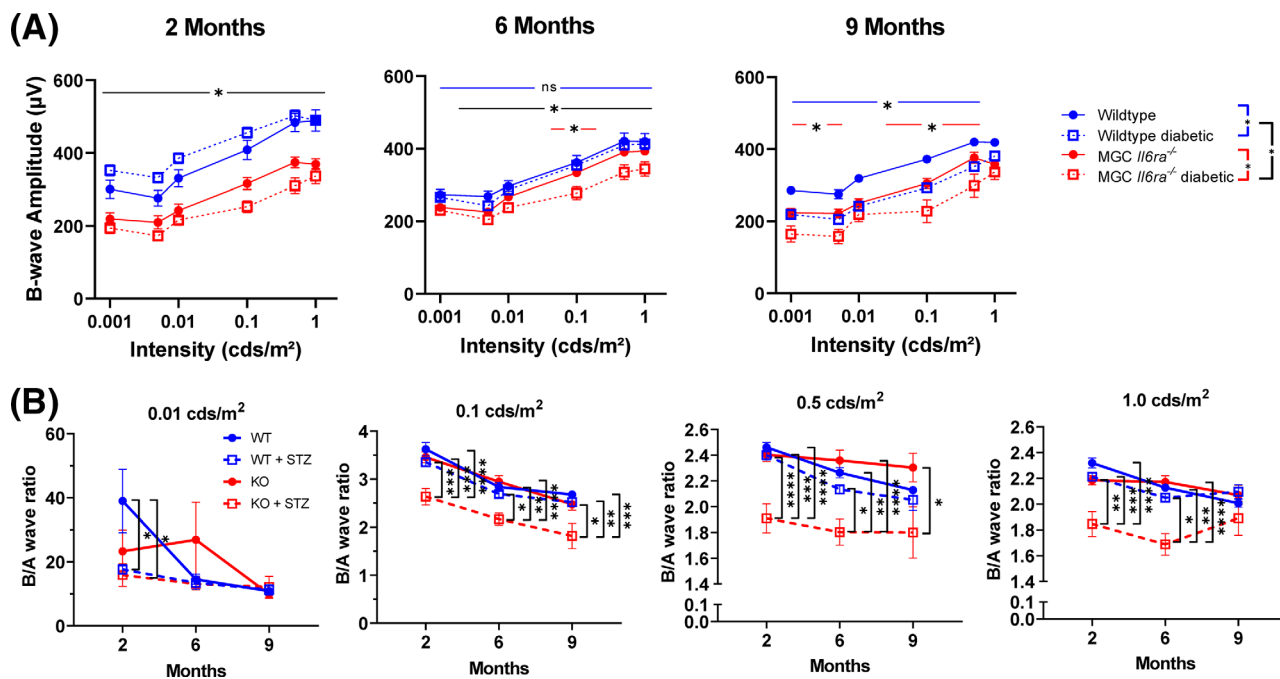


FIGURE 4. Diabetic MGC *Il6ra*^{-/-} mice have earlier scotopic ERG response and show a significant reduction in the B-wave/A-wave ratio. (A) Scotopic B-wave amplitudes and (B) B-wave/A-wave ratios of wildtype and MGC *Il6ra*^{-/-} mice with and without diabetes at 2, 6, and 9 months of diabetes. Graphed as mean ± SEM, *n* = 12 to 20 eyes from 6 to 10 mice per time point, per group; **P* < 0.05, ***P* < 0.01, ****P* < 0.001, *****P* < 0.0001; ns = not significant.

wildtype diabetic) at the same disease duration. This difference persisted throughout the length of the study, as diabetic MGC *Il6ra*^{-/-} mice had significantly thinner retinas than wildtype diabetic mice at 6 months (−12.0 µm, *P* = 0.002 versus wildtype diabetic) and 9 months (−5.0 µm, *P* = 0.040 versus wildtype diabetic). Representative images of SD-OCT

segmentation from 2-, 6-, and 9-month diabetic retinas are included in Supplementary Figure S1A–C.

We also observed significant thinning of the INL of diabetic MGC *Il6ra*^{-/-} mice at 2 months (−3.4 µm, *P* = 0.002 versus control), 6 months (−4.5 µm, *P* < 0.001 versus control), and 9 months (−3.7 µm, *P* < 0.001 versus control),

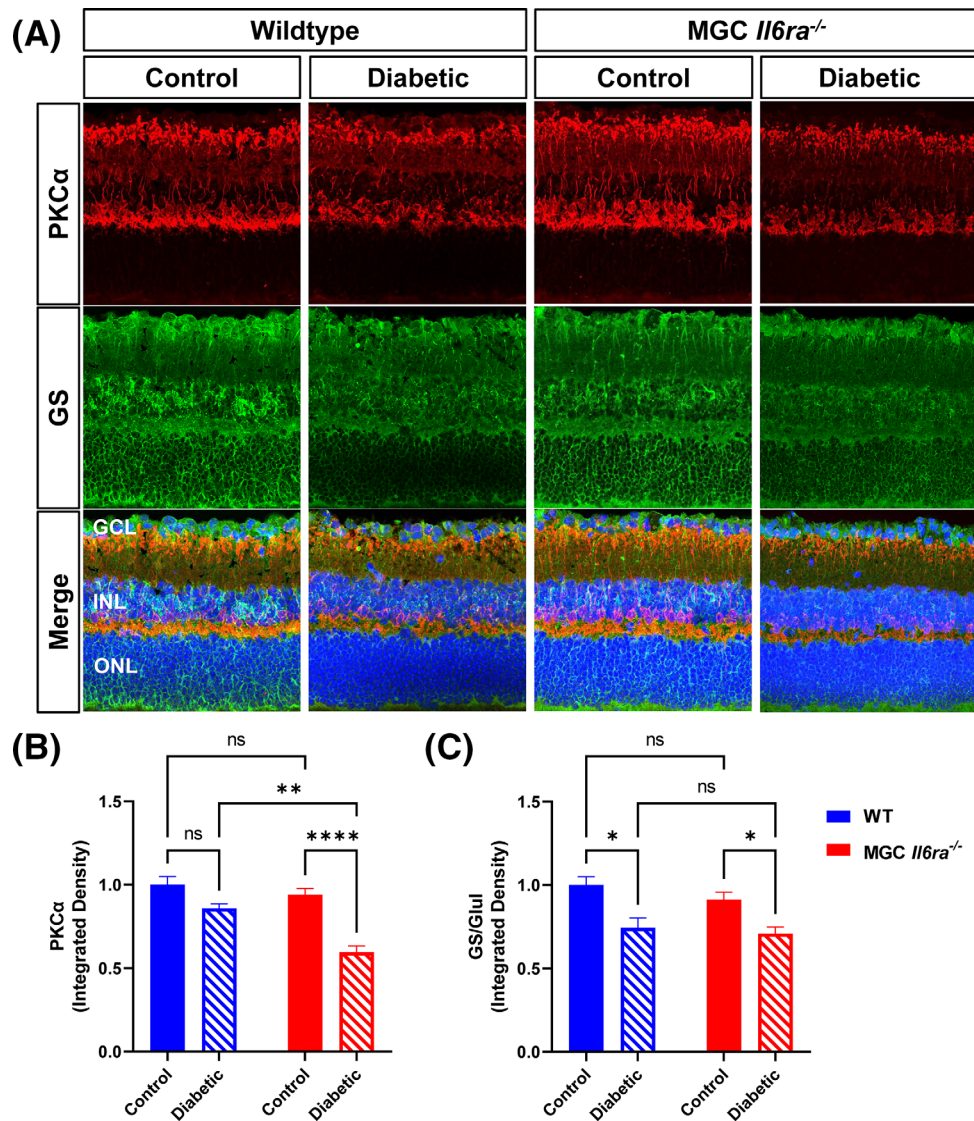


FIGURE 5. Diabetic MGC *Il6ra*^{-/-} mice show significant loss of bipolar neurons after 9 months of diabetes. (A) Expression of bipolar neuron marker PKC α (red), MGC marker GS (green), and DAPI nuclear stain (blue) at 9 months. Integrated pixel density for (B) PKC α and (C) GS quantified with ImageJ. Graphed as mean \pm SEM, $n = 4$ to 5 images/mouse/group; * $P < 0.05$, ** $P < 0.01$, **** $P < 0.0001$; ns = not significant. Ganglion cell layer (GCL), inner nuclear layer (INL), and outer nuclear layer (ONL).

whereas there was no significant change in INL thickness in diabetic wildtype mice until 9 months ($-2.6 \mu\text{m}$, $P < 0.001$ versus control; Fig. 3B). The changes observed in the INL account for much of the change in total retinal thickness in diabetic mice across all time points, whereas other retinal layers do not appear to follow this trend (Supplementary Fig. S2).

Diabetic MGC *Il6ra*^{-/-} Mice Have Significantly Reduced Scotopic ERG Response Earlier Than Wildtype Mice

Scotopic ERG responses at increasing flash intensities were recorded in all mice at 2, 6, and 9 months of diabetes to assess changes in retinal function. We observed a small baseline difference between genotypes at 2 months, but this difference between wildtype controls and MGC *Il6ra*^{-/-}

controls was not seen at 6 months or 9 months (Fig. 4A). We did not observe any difference between diabetic mice and their respective controls at 2 months, but, by 6 months, the diabetic MGC *Il6ra*^{-/-} mice showed a significant reduction in B-wave amplitude relative to diabetic wildtype mice. After 9 months of diabetes, diabetic mice from both genotypes showed the expected reduction in B-wave amplitude consistent with disease progression. Representative waveforms and all other supplemental data for scotopic and photopic ERG at 2, 6, and 9 months of diabetes are included in Supplementary Figures 3 and 4, respectively.

Further analysis of the B-wave/A-wave ratio over time showed a notable difference between diabetic MGC *Il6ra*^{-/-} mice and all other groups, most clearly seen at higher flash intensities (0.1, 0.5, and 1.0 cds/m^2 ; Fig. 4B). This difference was observed in both early (2 months) and late (9 months) disease. Changes to the B-wave/A-wave ratio reportedly correspond to changes within the inner retina,⁴⁵ suggesting

that the scotopic ERG changes observed in diabetic MGC *Il6ra*^{-/-} mice are likely not due to photoreceptor dysfunction, but instead due to distal neural retinal cells.

MGC *Il6ra*^{-/-} Mice Show Significant Bipolar Neuron Loss After 9 Months of Diabetes

The INL changes observed by OCT and ERG implicating the neural retina prompted us to assess the density of MGCs and bipolar neurons after 9 months of diabetes by co-staining retinal sections for MGC marker glutamine synthetase (GS) and bipolar neuron marker protein kinase C alpha (PKC α ; Fig. 5A). Quantification of immunofluorescence showed a significant decrease in PKC α intensity only in the diabetic MGC *Il6ra*^{-/-} mice, which was significantly lower than both MGC *Il6ra*^{-/-} controls (0.59 vs. 0.94, $P < 0.001$) and diabetic wildtype mice (0.59 vs. 0.86, $P = 0.002$; Fig. 5B). Interestingly, the MGC marker, GS, was significantly reduced in both diabetic wildtype (0.74 vs. 1.0, $P = 0.016$) and diabetic MGC *Il6ra*^{-/-} mice (0.71 vs. 0.91, $P = 0.047$), but there were no significant differences in GS levels between the two genotypes (Fig. 5C). These findings suggest that IL-6 cis-signaling in MGCs contributes to bipolar neuron health and that loss of *Il6ra* in MGCs reduces MGC-mediated neuroprotection of bipolar neurons in the diabetic retina.

DISCUSSION

Our laboratory has studied the role of IL-6 trans-signaling in the pathogenesis of DR, and our published work using human serum samples, retinal ECs, and diabetic mice have established an important role for IL-6 trans-signaling in endothelial barrier dysfunction, inflammation, and oxidative stress in the retina.^{16,24,46-49} Our recent work has focused primarily on the use of the fused chimera protein, sgp130Fc, an experimental biologic drug consisting of sgp130 fused with the constant (Fc) region of IgG1, which serves as a selective inhibitor of IL-6 trans-signaling 10-100 times more potent than endogenous sgp130.⁵⁰ Among our major findings, we have observed that selective inhibition of IL-6 trans-signaling in STZ-induced diabetic C57BL/6J mice significantly reduced retinal oxidative stress and oxidative damage, as measured by levels of malondialdehyde (MDA), dihydroxyethidium (DHE), and 8-hydroxy-2-deoxyguanosine (8-OHdG).²⁴ These *in vivo* effects of sgp130Fc treatment extended across all layers of the retina, which led us to broaden the scope of our studies beyond ECs to explore potential associations between IL-6 trans-signaling and other retinal cell types.

MGCs are specialized glial cells that play important roles in maintaining retinal homeostasis and are the major source of VEGF production, a critical contributor to DR pathology, in the mature retina.⁵¹⁻⁵³ MGCs are also the major retinal cell type expressing the membrane-bound IL-6 receptor, meaning that these cells are capable of both IL-6 cis- and trans-signaling and are likely to be affected by any disruption of the IL-6 cis-trans balance within the retina. Although intriguing, this complicates the differentiation of cis- and trans-signaling in this cell type. Trans-signaling can be selectively inhibited with sgp130Fc treatment to produce a “cis-signaling only” experimental model, but there are currently no selective inhibitors of IL-6 cis-signaling. Existing anti-IL-6 therapies targeting IL-6 (siltuximab) or IL-6R (tocilizumab) are global inhibitors that block both forms of signaling. As

previously discussed, we have developed an MGC-specific *Il6ra*^{-/-} mouse in which IL-6 cannot activate cis-signaling in MGCs, and, therefore, all IL-6 activity in these cells can occur only through IL-6 trans-signaling. We have verified that mIL-6R expression is unaffected in other tissues, such as the liver and spleen, and that systemic sIL-6R expression is retained, as well as the baseline retinal function of this novel strain.⁴⁴

To delineate the precise functions of IL-6 cis-signaling in MGCs, we induced diabetes in mice using STZ and monitored disease progression using funduscopy, FA, SD-OCT, and ERG in a longitudinal study. Whereas molecular, neuronal, and vascular changes could be detected in STZ-induced diabetic mice within 2 months of hyperglycemia, functional changes become evident around 6 to 9 months.⁵⁴⁻⁵⁷ We and others have reported changes at 2 months of hyperglycemia, including increased VEGF levels,⁵⁸ increased oxidative stress,⁴⁸ retinal superoxide generation,⁵⁹ increased leukocyte number,⁶⁰ leukostasis,⁶¹ and increased vessel leakage.⁶² Over a period of 8 to 9 months of diabetes, STZ mice develop microvascular changes in the retina that are consistent with clinically evident disease in humans with diabetes, including capillary degeneration,⁵⁴ thickening of the capillary basement membrane,⁵⁴ and capillary cell apoptosis.⁵⁵ Based on these reports, we chose time points at 2 months, 6 months, and 9 months of diabetes to evaluate both early stages and late (clinically evident DR) stages of this disease.

We postulate that IL-6 cis-signaling in MGCs is pivotal for maintaining retinal homeostasis. Consequently, diabetic MGC *Il6ra*^{-/-} mice lacking cis-signaling would likely experience retinal pathology at an earlier stage compared to diabetic wildtype mice, which are susceptible to the effects of both IL-6 cis- and trans-signaling. Our results demonstrate that diabetic MGC *Il6ra*^{-/-} mice exhibit retinal thinning much earlier in disease progression than wildtype mice and that much of this thinning is the result of volume loss in the INL. Remarkably, significant thinning of the INL in diabetic MGC *Il6ra*^{-/-} mice was observed as early as 2 months, whereas, in wildtype mice, significant thinning was not seen until 9 months, representing late-stage DR. This layer of the retina contains the cell bodies of MGCs, bipolar neurons, amacrine cells, and horizontal cells,⁶³⁻⁶⁵ and immunofluorescence staining of retinal sections showed that MGC *Il6ra*^{-/-} mice have significant loss of bipolar neurons at 9 months of diabetes, as measured by staining for bipolar neuron marker PKC α . In our ERG studies, we also observed a significant decrease in the scotopic B-wave amplitude in diabetic MGC *Il6ra*^{-/-} mice relative to diabetic wildtype mice. The B-wave corresponds to the depolarization of bipolar neurons during visual signal transmission, and dysfunction of this response aligns with the INL thinning and bipolar neuron loss observed by SD-OCT and immunofluorescence. In summary, these findings strongly indicate that IL-6 cis-signaling plays a significant role in MGC-mediated neuroprotection during the early stages of diabetes. Additionally, a disruption in the IL-6 cis-trans balance may expedite the onset or progression of pathology in the diabetic retina.

We previously characterized this knockout strain relative to controls and observed no significant changes in total retinal thickness or ERG response at baseline.⁴⁴ In this follow-up study, a decrease in ONL thickness was noted in both wildtype and knockout control mice at 9 months compared to 2 months (data not shown), likely due to non-pathologic aging. Interestingly, non-diabetic MGC *Il6ra*^{-/-} mice also

exhibited significant ONL thinning across all time points compared to wildtype controls. Previous studies focusing on retinal degeneration have demonstrated that MGCs have the ability to phagocytose apoptotic or dead photoreceptor cells, which are located in the ONL;⁶⁶ however, decreased ONL thickness in MGC *Il6ra*^{-/-} mice is most likely not due to mutations associated with retinal degeneration phenotypes, as we have confirmed that this strain does not possess the mutant *rd1*, *rd8*, or *nob5* alleles of *Pde6b*, *Crb1*, and *Gpr179*, respectively.⁴⁴ The loss of IL-6 cis-signaling in MGCs may have some unclear effect on photoreceptors, possibly due to altered juxtacrine signaling between MGCs in the INL and photoreceptors in the ONL, potentially leading to reduced support for photoreceptors in MGC *Il6ra*^{-/-} retina. Further investigation is needed to determine whether the loss of IL-6 cis-signaling in MGCs significantly impacts photoreceptor viability in this strain at baseline.

Of clinical significance, disorganization of the INL reportedly has a substantial impact on visual acuity.⁶⁷⁻⁶⁹ Studies in patients with type 1 diabetes have reported selective thinning of the INL without clinically observable signs of DR, suggesting an early neurodegenerative component to DR independent of vascular pathology, yet the mechanisms underlying these changes have not yet been identified.⁷⁰ Another study found an increase in bipolar neuron apoptosis in diabetic rats subsequent to anti-VEGF antibody administration. This effect is attributed to reduced activity of the neuroprotective phosphoinositide 3-kinase (PI3K)/Akt signaling pathway downstream of the VEGF receptor.⁷¹ Interestingly, the PI3K/Akt signaling pathway, along with the signal transducer and activator of transcription 3 (Stat3) and mitogen activated protein kinase/extracellular signal-related kinases (MAPK/ERK) pathways, can also be activated downstream of IL-6 signaling,⁷² but the activation of these pathways downstream of the IL-6 receptor can vary across different cell types. Therefore, additional studies are needed to assess IL-6 cis-signaling-induced activation of PI3K/Akt in MGCs and its potential neuroprotective effects.

In conclusion, our findings suggest that IL-6 cis-signaling in MGCs may play a novel neuroprotective role in the bipolar neurons and the inner nuclear layer in DR. These results emphasize the critical need to distinguish between IL-6 cis- and trans-signaling pathways in DR, as current evidence suggests the two pathways have distinct and contrasting functions. Our results also provide further support for the potential use of selective IL-6 trans-signaling inhibitors in DR, as experimental therapies like sgp130Fc may help mitigate the damage induced by trans-signaling without affecting the neuroprotective functions of IL-6 cis-signaling.

Acknowledgments

Supported by the National Institutes of Health, National Eye Institute (Bethesda, MD, USA) R01 grant # R01-EY026936 awarded to Shruti Sharma, PhD, and grant # P30-EY031631 Center Core Grant for Vision Research.

Disclosure: **J. Glass**, None; **R.L. Robinson**, None; **G. Greenway**, None; **G. Jones**, None; **S. Sharma**, None

References

- Gabay C. Interleukin-6 and chronic inflammation. *Arthritis Res Ther*. 2006;8(Suppl 2):S3.
- Rincon M. Interleukin-6: from an inflammatory marker to a target for inflammatory diseases. *Trends Immunol*. 2012;33:571-577.
- Koleva-Georgieva DN, Sivkova NP, Terzieva D. Serum inflammatory cytokines IL-1 β , IL-6, TNF- α and VEGF have influence on the development of diabetic retinopathy. *Folia Medica*. 2011;53:44-50.
- Mocan MC, Kadayifcilar S, Eldem B. Elevated intravitreal interleukin-6 levels in patients with proliferative diabetic retinopathy. *Can J Ophthalmol*. 2006;41:747-752.
- Funatsu H, Yamashita H, Shimizu E, Kojima R, Hori S. Relationship between vascular endothelial growth factor and interleukin-6 in diabetic retinopathy. *Retina*. 2001;21:469-477.
- Coughlin BA, Feenstra DJ, Mohr S. Müller cells and diabetic retinopathy. *Vis Res*. 2017;139:93-100.
- Rose-John S. IL-6 trans-signaling via the soluble IL-6 receptor: importance for the pro-inflammatory activities of IL-6. *Intl J Biologic Sci*. 2012;8:1237.
- Scheller J, Garbers C, Rose-John S. Interleukin-6: from basic biology to selective blockade of pro-inflammatory activities. *Semin Immunol*. 2014;26:2-12.
- Yego ECK, Vincent JA, Sarthy V, Busik JV, Mohr S. Differential regulation of high glucose-induced glyceraldehyde-3-phosphate dehydrogenase nuclear accumulation in Müller cells by IL-1 β and IL-6. *Invest Ophthalmol Vis Sci*. 2009;50:1920-1928.
- Grivennikov S, Karin E, Terzic J, et al. IL-6 and Stat3 are required for survival of intestinal epithelial cells and development of colitis-associated cancer. *Cancer Cell*. 2009;15:103-113.
- Scheller J, Chalaris A, Schmidt-Arras D, Rose-John S. The pro- and anti-inflammatory properties of the cytokine interleukin-6. *Biochimica et Biophysica Acta (BBA)-Molec Cell Res*. 2011;1813:878-888.
- Garbers C, Aparicio-Siegmund S, Rose-John S. The IL-6/gp130/STAT3 signaling axis: recent advances towards specific inhibition. *Curr Opin Immunol*. 2015;34:75-82.
- Rose-John S. Interleukin-6 signalling in health and disease. *F1000Res*. 2020;9:1-9.
- Jostock T, Müllberg J, Özbek S, et al. Soluble gp130 is the natural inhibitor of soluble interleukin-6 receptor transsignaling responses. *Eur J Biochem*. 2001;268:160-167.
- Becker C, Fantini MC, Schramm C, et al. TGF-beta suppresses tumor progression in colon cancer by inhibition of IL-6 trans-signaling. *Immunity*. 2004;21:491-501.
- Valle ML, Dworshak J, Sharma A, Ibrahim AS, Al-Shabrawey M, Sharma S. Inhibition of interleukin-6 trans-signaling prevents inflammation and endothelial barrier disruption in retinal endothelial cells. *Exp Eye Res*. 2019;178:27-36.
- Rose-John S. IL-6 trans-signaling via the soluble IL-6 receptor: importance for the pro-inflammatory activities of IL-6. *Int J Biol Sci*. 2012;8:1237-1247.
- Coughlin BA, Trombley BT, Mohr S. Interleukin-6 (IL-6) mediates protection against glucose toxicity in human Müller cells via activation of VEGF-A signaling. *Biochem Biophys Res Commun*. 2019;517:227-232.
- Sanchez RN, Chan CK, Garg S, et al. Interleukin-6 in retinal ischemia reperfusion injury in rats. *Invest Ophthalmol Vis Sci*. 2003;44:4006-4011.
- Leibinger M, Müller A, Gobrecht P, Diekmann H, Andreadaki A, Fischer D. Interleukin-6 contributes to CNS axon regeneration upon inflammatory stimulation. *Cell Death Dis*. 2013;4:e609.
- Chong DY, Boehlke CS, Zheng Q-D, Zhang L, Han Y, Zacks DN. Interleukin-6 as a photoreceptor neuroprotectant in an

- experimental model of retinal detachment. *Invest Ophthalmol Vis Sci.* 2008;49:3193–3200.
22. Sappington RM, Chan M, Calkins DJ. Interleukin-6 protects retinal ganglion cells from pressure-induced death. *Invest Ophthalmol Vis Sci.* 2006;47:2932–2942.
 23. Yego ECK, Vincent JA, Sarthy V, Busik JV, Mohr S. Differential regulation of high glucose-induced glyceraldehyde-3-phosphate dehydrogenase nuclear accumulation in Müller cells by IL-1 β and IL-6. *Invest Ophthalmol Vis Sci.* 2009;50:1920–1928.
 24. Robinson R, Srinivasan M, Shanmugam A, et al. Interleukin-6 trans-signaling inhibition prevents oxidative stress in a mouse model of early diabetic retinopathy. *Redox Biol.* 2020;34:101574.
 25. Rojas M, Zhang W, Lee DL, et al. Role of IL-6 in angiotensin II-induced retinal vascular inflammation. *Invest Ophthalmol Vis Sci.* 2010;51:1709–1718.
 26. Rojas MA, Zhang W, Xu Z, Nguyen DT, Caldwell RW, Caldwell RB. Interleukin 6 has a critical role in diabetes-induced retinal vascular inflammation and permeability. *Invest Ophthalmol Vis Sci.* 2011;52:1003.
 27. Rübssam A, Parikh S, Fort PE. Role of inflammation in diabetic retinopathy. *Intl J Molec Sci.* 2018;19:942.
 28. Coorey NJ, Shen W, Chung SH, Zhu L, Gillies MC. The role of glia in retinal vascular disease. *Clinic Exp Optom.* 2012;95:266–281.
 29. Bringmann A, Pannicke T, Grosche J, et al. Müller cells in the healthy and diseased retina. *Prog Retin Eye Res.* 2006;25:397–424.
 30. Muto T, Tien T, Kim D, Sarthy VP, Roy S. High glucose alters Cx43 expression and gap junction intercellular communication in retinal Müller cells: promotes Müller cell and pericyte apoptosis. *Invest Ophthalmol Vis Sci.* 2014;55:4327–4337.
 31. Roy S, Kim D, Lim R. Cell-cell communication in diabetic retinopathy. *Vis Res.* 2017;139:115–122.
 32. Ahmad I, Del Debbio CB, Das AV, Parameswaran S. Müller glia: a promising target for therapeutic regeneration. *Invest Ophthalmol Vis Sci.* 2011;52:5758–5764.
 33. Newman E, Reichenbach A. The Müller cell: a functional element of the retina. *Trends Neurosci.* 1996;19:307–312.
 34. Tout S, Chan-Ling T, Hollander H, Stone J. The role of Müller cells in the formation of the blood-retinal barrier. *Neuroscience.* 1993;55:291–301.
 35. Abukawa H, Tomi M, Kiyokawa J, et al. Modulation of retinal capillary endothelial cells by Müller glial cell-derived factors. *Mol Vis.* 2009;15:451–457.
 36. Roy S, Kern TS, Song B, Stuebe C. Mechanistic insights into pathological changes in the diabetic retina: implications for targeting diabetic retinopathy. *Am J Pathol.* 2017;187:9–19.
 37. Duh EJ, Sun JK, Stitt AW. Diabetic retinopathy: current understanding, mechanisms, and treatment strategies. *JCI Insight.* 2017;2:1–13.
 38. Walker RJ, Steinle JJ. Role of β -adrenergic receptors in inflammatory marker expression in Müller cells. *Invest Ophthalmol Vis Sci.* 2007;48:5276–5281.
 39. Walker RJ, Anderson NM, Bahouth S, Steinle JJ. Silencing of insulin receptor substrate-1 increases cell death in retinal Müller cells. *Molec Vis.* 2012;18:271.
 40. Bibliowicz J, Tittle RK, Gross JM. Toward a better understanding of human eye disease: insights from the zebrafish, *Danio rerio*. *Prog Molec Biol Transl Sci.* 2011;100:287–330.
 41. Xia C-h, Yablonka-Reuveni Z, Gong X. LRP5 is required for vascular development in deeper layers of the retina. *PLoS One.* 2010;5:e11676.
 42. Dyer MA, Cepko CL. Control of Müller glial cell proliferation and activation following retinal injury. *Nature Neurosci.* 2000;3:873–880.
 43. Kim D, Lewis CS, Sarthy VP, Roy S. High-glucose-induced Rab20 upregulation disrupts gap junction intercellular communication and promotes apoptosis in retinal endothelial and Müller cells: implications for diabetic retinopathy. *J Clin Med.* 2020;9:3710.
 44. Robinson R, Glass J, Sharma A, Sharma S. Generation and characterization of a Müller-glial-cell-specific *Il6ra* knockout mouse to delineate the effects of IL-6 trans-signaling in the retina. *Sci Rep.* 2022;12:17626.
 45. Hombrebueno JR, Chen M, Penalva RG, Xu H. Loss of synaptic connectivity, particularly in second order neurons is a key feature of diabetic retinal neuropathy in the Ins2Akita mouse. *PLoS One.* 2014;9:e97970.
 46. Glass J, Robinson R, Lee T-J, Sharma A, Sharma S. Interleukin-6 trans-signaling mediated regulation of paracellular permeability in human retinal endothelial cells. *Intl J Transl Med.* 2021;1:137–153.
 47. Robinson R, Brown D, Churchwell L, et al. RNA-Seq analysis reveals gene expression changes induced by IL-6 trans-signaling activation in retinal endothelial cells. *Cytokine.* 2020;139:155375.
 48. Robinson R, Youngblood H, Iyer H, et al. Diabetes Induced alterations in murine vitreous proteome are mitigated by IL-6 trans-signaling inhibition. *Invest Ophthalmol Vis Sci.* 2020;61:2.
 49. Sharma S, Purohit S, Sharma A, et al. Elevated serum levels of soluble TNF receptors and adhesion molecules are associated with diabetic retinopathy in patients with type-1 diabetes. *Mediators Inflamm.* 2015;2015:160–167.
 50. Jostock T, Mullberg J, Ozbek S, et al. Soluble gp130 is the natural inhibitor of soluble interleukin-6 receptor transsignaling responses. *Eur J Biochem.* 2001;268:160–167.
 51. Carpi-Santos R, de Melo Reis RA, Gomes FCA, Calaza KC. Contribution of Müller cells in the diabetic retinopathy development: focus on oxidative stress and inflammation. *Antioxidants.* 2022;11:617.
 52. Wang J, Xu X, Elliott MH, Zhu M, Le Y-Z. Müller cell-derived VEGF is essential for diabetes-induced retinal inflammation and vascular leakage. *Diabetes.* 2010;59:2297–2305.
 53. Bai Y, Jx Ma, Guo J, et al. Müller cell-derived VEGF is a significant contributor to retinal neovascularization. *J Pathol.* 2009;219:446–454.
 54. Zheng L, Du Y, Miller C, et al. Critical role of inducible nitric oxide synthase in degeneration of retinal capillaries in mice with streptozotocin-induced diabetes. *Diabetologia.* 2007;50:1987–1996.
 55. Feit-Leichman RA, Kinouchi R, Takeda M, et al. Vascular damage in a mouse model of diabetic retinopathy: relation to neuronal and glial changes. *Invest Ophthalmol Vis Sci.* 2005;46:4281–4287.
 56. Gaucher D, Chiappore JA, Paques M, et al. Microglial changes occur without neural cell death in diabetic retinopathy. *Vis Res.* 2007;47:612–623.
 57. Berkowitz BA, Gadianu M, Bissig D, Kern TS, Roberts R. Retinal ion regulation in a mouse model of diabetic retinopathy: natural history and the effect of Cu/Zn superoxide dismutase overexpression. *Invest Ophthalmol Vis Sci.* 2009;50:2351–2358.
 58. Mima A, Qi W, Hiraoka-Yamamoto J, et al. Retinal not systemic oxidative and inflammatory stress correlated with VEGF expression in rodent models of insulin resistance and diabetes. *Invest Ophthalmol Vis Sci.* 2012;53:8424–8432.
 59. Tang J, Du Y, Petrash JM, Sheibani N, Kern TS. Deletion of aldose reductase from mice inhibits diabetes-induced retinal capillary degeneration and superoxide generation. *PLoS One.* 2013;8:e62081.

60. Kubota S, Ozawa Y, Kurihara T, et al. Roles of AMP-activated protein kinase in diabetes-induced retinal inflammation. *Invest Ophthalmol Vis Sci.* 2011;52:9142–9148.
61. Li G, Tang J, Du Y, Lee CA, Kern TS. Beneficial effects of a novel RAGE inhibitor on early diabetic retinopathy and tactile allodynia. *Mol Vis.* 2011;17:3156–3165.
62. Kim YH, Kim YS, Roh GS, Choi WS, Cho GJ. Resveratrol blocks diabetes-induced early vascular lesions and vascular endothelial growth factor induction in mouse retinas. *Acta Ophthalmol.* 2012;90:e31–e37.
63. Masri RA, Weltzien F, Purushothuman S, Lee SC, Martin PR, Grünert U. Composition of the inner nuclear layer in human retina. *Invest Ophthalmol Vis Sci.* 2021;62:22.
64. Strettoi E, Masland RH. The organization of the inner nuclear layer of the rabbit retina. *J Neurosci.* 1995;15:875–888.
65. Lee EJ, Mann LB, Rickman DW, Lim EJ, Chun MH, Grzywacz NM. AII amacrine cells in the distal inner nuclear layer of the mouse retina. *J Compar Neurol.* 2006;494:651–662.
66. Sakami S, Imanishi Y, Palczewski K. Müller glia phagocytose dead photoreceptor cells in a mouse model of retinal degenerative disease. *FASEB J.* 2019;33:3680.
67. Sun JK, Lin MM, Lammer J, et al. Disorganization of the retinal inner layers as a predictor of visual acuity in eyes with center-involved diabetic macular edema. *JAMA Ophthalmol.* 2014;132:1309–1316.
68. Sun JK, Radwan SH, Soliman AZ, et al. Neural retinal disorganization as a robust marker of visual acuity in current and resolved diabetic macular edema. *Diabetes.* 2015;64:2560–2570.
69. Das R, Spence G, Hogg RE, Stevenson M, Chakravarthy U. Disorganization of inner retina and outer retinal morphology in diabetic macular edema. *JAMA Ophthalmol.* 2018;136:202–208.
70. Van Dijk HW, Kok PH, Garvin M, et al. Selective loss of inner retinal layer thickness in type 1 diabetic patients with minimal diabetic retinopathy. *Invest Ophthalmol Vis Sci.* 2009;50:3404–3409.
71. Park H-YL, Kim JH, Park CK. Neuronal cell death in the inner retina and the influence of vascular endothelial growth factor inhibition in a diabetic rat model. *Am J Pathol.* 2014;184:1752–1762.
72. Zegeye MM, Lindkvist M, Fälker K, et al. Activation of the JAK/STAT3 and PI3K/AKT pathways are crucial for IL-6 trans-signaling-mediated pro-inflammatory response in human vascular endothelial cells. *Cell Commun Signal.* 2018;16:1–10.